

Indirect Gradient Matching for Adversarial Robust Distillation

Hongsin Lee* Seungju Cho* Changick Kim
 Korea Advanced Institute of Science and Technology
 {hongsin04, joyga, changick}@kaist.ac.kr

Abstract

Adversarial training significantly improves adversarial robustness, but superior performance is primarily attained with large models. This substantial performance gap for smaller models has spurred active research into adversarial distillation (AD) to mitigate the difference. Existing AD methods leverage the teacher’s logits as a guide. In contrast to these approaches, we aim to transfer another piece of knowledge from the teacher, the input gradient. In this paper, we propose a distillation module termed Indirect Gradient Distillation Module (IGDM) that indirectly matches the student’s input gradient with that of the teacher. We hypothesize that students can better acquire the teacher’s knowledge by matching the input gradient. Leveraging the observation that adversarial training renders the model locally linear on the input space, we employ Taylor approximation to effectively align gradients without directly calculating them. Experimental results show that IGDM seamlessly integrates with existing AD methods, significantly enhancing the performance of all AD methods. Particularly, utilizing IGDM on the CIFAR-100 dataset improves the AutoAttack accuracy from 28.06% to 30.32% with the ResNet-18 model and from 26.18% to 29.52% with the MobileNetV2 model when integrated into the SOTA method without additional data augmentation. The code will be made available.

1. Introduction

Recently, adversarial attacks have revealed the vulnerabilities of deep learning-based models [4, 16, 29], raising critical concerns in safety-important applications [17, 28, 36]. Thus, much research has been done on defense technologies to make deep learning more reliable [5, 7, 12, 23, 42, 46]. Among adversarial defense mechanisms, adversarial training is one of the most effective methods to enhance adversarial robustness [2, 31, 40]. However, there is a significant performance gap between large and small models in adversarial training. Since light models with less computational complexity are preferred in practical applications, increasing the robustness of light models is necessary.

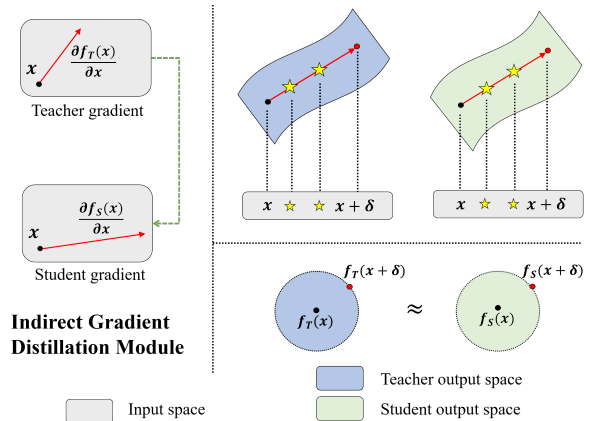


Figure 1. Conceptual diagram of Indirect Gradient Distillation Module. We match the gradient in the input space with knowledge distillation. Since adversarial robust models are locally linear, matching the gradient has the effect of matching the output points of the surrounding input marked with ‘stars’, as illustrated in the top right figure. Consequently, gradient matching involves matching the teacher and student point by point in the output space, as depicted in the bottom right.

To address this, adversarial training incorporates distillation methodologies which are commonly employed to boost the performance of light or small models [15, 20, 47, 49].

In the teacher-student architecture of knowledge distillation, prevailing methods leverage the teacher’s features or logits [19, 21, 24, 44]. Adversarial distillation (AD) approaches extend this paradigm by incorporating the teacher’s logits as a guide within their adversarial training framework [15, 20, 30, 47, 49]. Recent studies have specifically focused on tailoring the inner maximization problem of adversarial training, particularly by involving the teacher model in the generation of adversarial examples [20, 49]. In this paper, we exploit another knowledge of teachers: input gradient, which is helpful in the outer minimization of adversarial training.

We observe that adversarial training makes models locally linear on the input space and this linearity starts from the early stage of training. The property of being locally

linear enables the application of the first-order Taylor expansion, facilitating the alignment of gradients between the teacher and student models without the need for explicit gradient calculations. We demonstrate that matching input gradients between teacher and student contributes to point-to-point alignment, allowing the student to better imitate the robust teacher. In the top right of Fig. 1, if the input gradients between the teacher and the student match as depicted in the red line, then the output of the points located on the red line, denoted as *stars*, will also match. We show that the output of random points around x also becomes similar to the teacher as illustrated in the bottom right of Fig. 1. This alignment causes the student to mimic the teacher and reduces the capacity gap between teacher and student.

In this paper, we propose *Indirect Gradient Distillation Module* (IGDM), which indirectly aligns the student’s gradient with that of the teacher. Since existing AD methods are mainly designed to match only logits, IGDM can be used in conjunction with them. Through extensive experimental results, we verify that our method successfully complements the robustness of existing AD methods.

Our contributions are as follows:

- We propose a methodology to transfer the gradient information from the teacher to the student through the exploitation of the local linearity inherent in adversarial training. This stands in contrast to prevailing AD methods, which primarily concentrate on the distillation of logits.
- Based on the analysis, we propose the Indirect Gradient Distillation Module (IGDM), which indirectly distills the gradient information. Its modular design allows easy integration into existing AD methods.
- IGDM notably improves robustness across various attack scenarios, demonstrating significant AutoAttack robustness trained on the CIFAR-100 dataset: 30.32% on ResNet-18 and 29.52% on MobileNetV2. Furthermore, our module is effective even without employing the teacher model in the inner maximization.

2. Related work

2.1. Adversarial Training

Adversarial training (AT) involves generating adversarial examples during the training process to enhance model robustness. The objective function of AT is a minimization-maximization problem as follows.

$$\min_{\mathbf{w}} \mathbb{E}_{(\mathbf{x}, y) \sim D} \left(\max_{\|\delta\|_p \leq \epsilon} [l_{obj}(\mathbf{x} + \delta, y)] \right), \quad (1)$$

where \mathbf{w} is model parameters, D is a data distribution of \mathbf{x} and corresponding labels y , δ is perturbation causing

the largest loss within l_p norm of ϵ , and l_{obj} is an objective function such as cross-entropy loss. Multi-step PGD attack [29] is commonly utilized to solve the inner maximization problem of Eq. (1), and various regularization loss functions have been introduced for the outer minimization problem. TRADES [45] incorporates the Kullback-Leibler (KL) divergence loss between the predictions of clean and adversarial images. MART [38] introduces per-sample weights based on the confidence of each sample. Due to their simplicity and effectiveness, TRADES and MART are commonly used as baseline methods in adversarial training [3, 22, 23, 34, 40, 41]. Moreover, several strategies such as data augmentation [27, 32], and diverse loss functions [41], have been introduced.

Although defending against strong adversarial attack strategies [1, 9, 10] is challenging, highly robust models have also been developed. Low Temperature Distillation (LTD) [6] points out the shortcomings of one-hot labels in adversarial training and advocates the use of soft labels as an alternative approach. Better Diffusion Models for Adversarial Training (BDM-AT) [39] explores methods for the more efficient utilization of diffusion models within the context of adversarial training. Improved Kullback–Leibler Adversarial Training (IKL-AT) [11] inspects the mechanism of KL divergence loss and proposes the Decoupled Kullback-Leibler divergence loss. However, since these models utilize large architectures, there is a need to improve adversarial robustness in smaller models.

2.2. Adversarial Robust Distillation

Adversarial Robustness Distillation (ARD) [15] is the first study to propose the AD. ARD reveals that students can more effectively acquire robustness when guided by a robust teacher within an adversarial training framework. RSLAD [49] highlights the significance of the smooth logit learned by the teacher in robust distillation. It diverges from ARD by eliminating the student’s cross-entropy loss, relying solely on guidance from the teacher’s output. Furthermore, RSLAD incorporates teachers into the adversarial image generation process. AdaAD [20] generates more sophisticated adversarial images through the integration of the teacher during the inner maximization process. Introspective Adversarial Distillation (IAD) [47] concentrates on assessing the reliability of the teacher and introduces a confidence score of the information provided by the teacher. Previous AD methods utilize the teacher’s logits as a guide, but our approach incorporates the distillation of gradient information as well.

2.3. Gradient Distillation

In knowledge distillation, gradient information has been used in various ways [14, 26, 35, 48], computed in either input space or weight space. For example, an exploration of

the diversity among teacher models in the weight gradient space aids in identifying an optimal direction for training the student network [14]. Another study examines the capacity gap between teachers and students, focusing on the perspective of weight gradients similarity [48]. Conversely, input space gradients find applications in knowledge distillation for tasks such as object detection [26] or language model [35]. These methods all compute the gradient directly, which is different from our approach.

3. Method

In knowledge distillation, students attempt to emulate teachers by aligning their features or outputs with those of the teachers. However, the need for more comprehensive knowledge transfer arises in the context of adversarial robustness, given that adversaries introduce perturbations to input data. Consequently, the transfer of extensive knowledge from the input neighborhood becomes crucial. However, transferring knowledge of all points one by one is impractical due to the infinite number of vicinity points. To address this problem, we match the input gradients of the student and the teacher. This gradient alignment is essential in facilitating the student’s emulation of the teacher. The following sections elucidate how we can match the gradients without direct calculation.

3.1. Locally Linearity of Adversarial Training

Unlike natural training, adversarially trained models are capable of first-order Taylor expansion on the input. The output for small noise around \mathbf{x} can be expressed as follows.

$$f(\mathbf{x} + \epsilon) = \underbrace{f(\mathbf{x}) + \left(\frac{\partial f(\mathbf{x})}{\partial \mathbf{x}}\right)^T \epsilon}_{\text{first-order approximation}} + \underbrace{O(\|\epsilon\|^2)}_{\text{remainder}}, \quad (2)$$

where f is the model and ϵ is sufficiently small noise with the same dimension as the \mathbf{x} . To investigate the impact of the remainder, we compute the proportion occupied by the remainder in Eq. (2). Here, we apply uniform noise with a size of $8/255$ as the perturbation ϵ , which is a common size in adversarial attacks. We first examine the remainder proportion in an adversarially well-trained model: LTD [6], BDM-AT [39], and IKL-AT [11] where we summarized the performance in Table 1. In Fig. 2a, the remainder proportions are computed to be very small, with values of 0.012, 0.012, and 0.016 for three adversarially-trained models LTD, BDM-AT, and IKL-AT, respectively. In other words, $f(\mathbf{x} + \epsilon)$ can be approximated to the first-order Taylor expansion since the remainder proportion is negligible. Thus, we utilize this local linearity of the adversarially well-trained models.

Next, we investigate whether the model retains the local linearity in adversarial training, not in the case of a

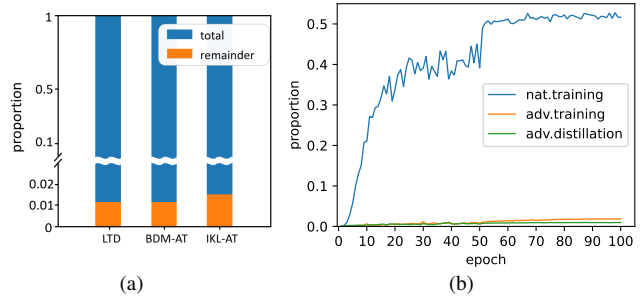


Figure 2. The proportion occupied by the remainder in Taylor expansion. The left side plots the remainder proportion of an adversarially robust teacher model, and the right side plots the proportion along with training epochs in natural training, adversarial training, and adversarial distillation.

fully-trained model. We test three training strategies: natural training, adversarial training via ten steps of PGD, and adversarial distillation [15] using the BDM-AT teacher. In Fig. 2b, the remainder proportion continuously increases in natural training, while it consistently remains small in both adversarial training and adversarial distillation. Therefore, employing first-order Taylor expansion is feasible during adversarial training and distillation procedures. In the following section, we demonstrate how the locally linear property enables the matching of input gradients between the teacher and the student.

3.2. Gradient Matching via Output Differences

For an input \mathbf{x} , we define \mathbf{x}_{ϵ_1} and \mathbf{x}_{ϵ_2} as follows:

$$\mathbf{x}_{\epsilon_1} = \mathbf{x} + \epsilon_1, \quad \mathbf{x}_{\epsilon_2} = \mathbf{x} + \epsilon_2, \quad (3)$$

where ϵ_1 and ϵ_2 represent small perturbations of the same dimension as the input \mathbf{x} . For adversarially trained or training model f , the output of \mathbf{x}_{ϵ_1} and \mathbf{x}_{ϵ_2} can be approximated using first-order Taylor expansion through the input space:

$$\begin{aligned} f(\mathbf{x}_{\epsilon_1}) &\approx f(\mathbf{x}) + \left(\frac{\partial f(\mathbf{x})}{\partial \mathbf{x}}\right)^T \epsilon_1, \\ f(\mathbf{x}_{\epsilon_2}) &\approx f(\mathbf{x}) + \left(\frac{\partial f(\mathbf{x})}{\partial \mathbf{x}}\right)^T \epsilon_2, \end{aligned} \quad (4)$$

where we neglect the remainder term based on the observations in Section 3.1. To extract and align the gradients between the student and the teacher models, we utilize the output differences as follows:

$$L = D(f_S(\mathbf{x}_{\epsilon_1}) - f_S(\mathbf{x}_{\epsilon_2}), f_T(\mathbf{x}_{\epsilon_1}) - f_T(\mathbf{x}_{\epsilon_2})), \quad (5)$$

where f_S and f_T represent the student and teacher models, while D denotes a distance metric like L2 or KL loss. This loss can be reformulated using Eq. (4) as follows:

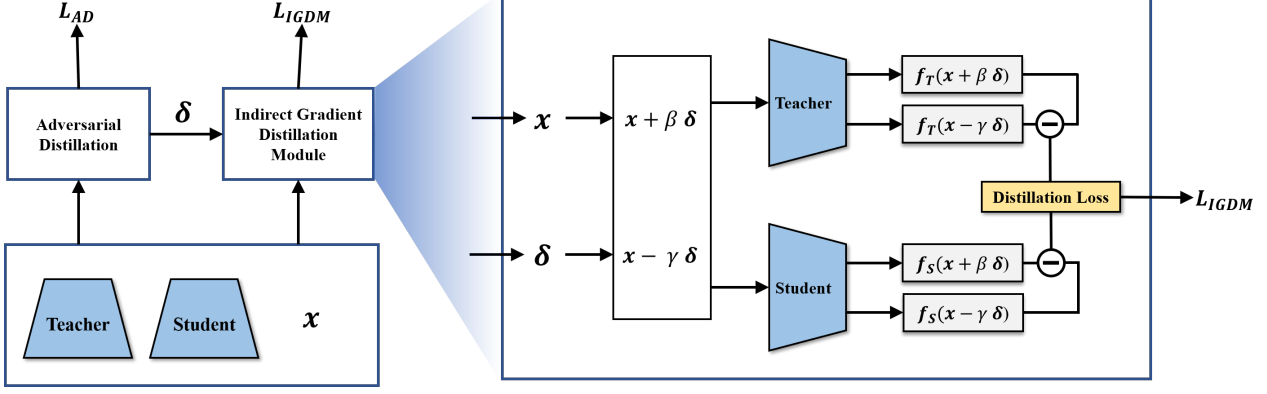


Figure 3. Summary diagram of AD with IGDM. IGDM indirectly obtains input gradients of both the teacher and the student by calculating output differences and perform distillation to match the gradients. IGDM can be seamlessly integrated with existing AD methods.

$$L = D \left(\left(\frac{\partial f_S(\mathbf{x})}{\partial \mathbf{x}} \right)^T (\epsilon_1 - \epsilon_2), \left(\frac{\partial f_T(\mathbf{x})}{\partial \mathbf{x}} \right)^T (\epsilon_1 - \epsilon_2) \right). \quad (6)$$

Since $\epsilon_1 - \epsilon_2$ is inner-producted on both sides within the distance metric, optimizing the given loss achieves the alignment of the gradients between the student and the teacher models, *i.e.*,

$$\frac{\partial f_S(\mathbf{x})}{\partial \mathbf{x}} \approx \frac{\partial f_T(\mathbf{x})}{\partial \mathbf{x}}. \quad (7)$$

3.3. Indirect Gradient Distillation Module (IGDM)

To effectively integrate the gradient matching through output differences into AD methods, we select the ϵ_1 and ϵ_2 as constant multiples of the adversary perturbation δ from the AD methods, *i.e.*, $\epsilon_1 - \epsilon_2 \propto \delta$. Since the adversarial perturbation δ closely aligns with the gradient direction, the inner product of gradient and $\epsilon_1 - \epsilon_2$ in Eq. (6) can be effectively increased with the adversarial perturbation. In other words, $\left(\frac{\partial f_S(\mathbf{x})}{\partial \mathbf{x}} \right)^T (\epsilon_1 - \epsilon_2) \propto \left(\frac{\partial f_S(\mathbf{x})}{\partial \mathbf{x}} \right)^T \delta$ remains large, facilitating the enhanced alignment of gradients using loss function in Eq. (6) during training. If $\epsilon_1 - \epsilon_2$ were random noise, its inner product would be zero when the noise is orthogonal to the gradient, thereby making no contribution to the alignment of gradients.

Finally, Indirect Gradient Distillation Module (IGDM) loss is formulated as:

$$L_{IGDM} = T(\alpha) \cdot D \left(f_S(\mathbf{x} + \beta\delta) - f_S(\mathbf{x} - \gamma\delta), f_T(\mathbf{x} + \beta\delta) - f_T(\mathbf{x} - \gamma\delta) \right). \quad (8)$$

Here, $T(\alpha)$ is a non-negative, increasing hyperparameter function throughout the training epochs, mitigating the risk of falling into the local minima in the initial training phases. Both β and γ are non-negative hyperparameters. Our model architecture is depicted in Fig. 3. Since IGDM complements the objective function by matching the gradients between the teacher and student models, the integration of

IGDM with other AD methods becomes feasible in the following manner:

$$l_{obj} = L_{AD} + L_{IGDM}, \quad (9)$$

where L_{AD} stands for the objective function of other AD methods such as ARD [15], RSLAD [49], AdaAD [20], etc.

3.4. Enhancing Teacher-Student Alignment through Gradient Matching

In this section, we elucidate the role of gradient matching in facilitating students to emulate their teachers. An underlying aim of knowledge distillation is to foster alignment between the teacher and the student. In AD, the alignment should take into account not only clean images but also adversarial images. For instance, RSLAD [49] attempts to match both clean and adversarial images by using the following objective function:

$$l_{obj} = \min_{\theta} [\text{KL}(S_{\theta}(\mathbf{x}), T(\mathbf{x})) + \text{KL}(S_{\theta}(\mathbf{x} + \delta), T(\mathbf{x}))]. \quad (10)$$

AdaAD [20] points out there is a non-negligible property of local variance on teacher model: for $\forall \delta_1 \neq \delta_2, T(\mathbf{x} + \delta_1) \neq T(\mathbf{x} + \delta_2)$. Therefore, to align the student and teacher under the local variance, AdaAD employs the following loss function.

$$l_{obj} = \min_{\theta} \text{KL}(S_{\theta}(\mathbf{x} + \delta), T(\mathbf{x} + \delta)). \quad (11)$$

In other words, AdaAD emphasizes matching between $T(\mathbf{x} + \delta)$ and $S(\mathbf{x} + \delta)$ where δ is a small perturbation.

While RSLAD and AdaAD explicitly try to match the output between teacher and student, IGDM implicitly matches teacher and student. We define point-wise distance $D(\mathbf{x}, \delta) = \|f_T(\mathbf{x} + \delta) - f_S(\mathbf{x} + \delta)\|$. Then given \mathbf{x} , the upper bound of $D(\mathbf{x}, \delta)$ for sufficiently small δ is as follows.

$$\begin{aligned}
D(\mathbf{x}, \delta) &\approx \left\| (f_T(\mathbf{x}) - f_S(\mathbf{x}) + \left(\frac{\partial f_T(\mathbf{x})}{\partial \mathbf{x}} - \frac{\partial f_S(\mathbf{x})}{\partial \mathbf{x}} \right)^T \delta \right\| \\
&\leq \|f_T(\mathbf{x}) - f_S(\mathbf{x})\| + \left\| \left(\frac{\partial f_T(\mathbf{x})}{\partial \mathbf{x}} - \frac{\partial f_S(\mathbf{x})}{\partial \mathbf{x}} \right)^T \delta \right\|,
\end{aligned} \tag{12}$$

where the inequality came out through the triangle inequality. We see that the distance $D(\mathbf{x}, \delta)$ is bounded by the output term and the gradient term. Hence, the better the gradient matching, the smaller the upper bound of $D(\mathbf{x}, \delta)$ becomes. Therefore, IGDM implicitly aligns the teacher and student in a points-wisely manner.

4. Experiments

We explain about experimental setup, followed by comparative performance evaluations of the proposed IGDM method against various AT and AD methods.

4.1. Settings

We utilized the CIFAR-10 and CIFAR-100 [25] datasets for our experiments. Random crop and random horizontal flip were applied, while other augmentations were not utilized. Our training methods encompassed conventional adversarial training methods (PGD-AT [29] and TRADES [45]), as well as adversarial distillation techniques including ARD [15], IAD [47], RSLAD [49], and AdaAD [20]. In our comparative analysis, we integrated IGDM into all of these methods, and we used shortened notations to represent the methods with IGDM. For example, when IGDM is combined with ARD, we denote it as **ARD + IGDM** or IGDM_{ARD} . We fixed the hyperparameters of all given methods used in the experiment as original paper, and detailed information is in the supplementary materials. Then, we only adjusted the hyperparameters of IGDM, α , β , and γ . For the surrogate loss of IGDM, we employed KL divergence loss, but using alternative surrogate losses, such as L1 and L2 loss, yields nearly indistinguishable results.

Teacher and Student Models We selected three teacher models including LTD [6], BDM-AT [39], and IKL-AT [11]. The LTD model is widely adopted in prior AD research, while the others have achieved high-ranking performance in RobustBench [8], demonstrating superior robustness against AutoAttack [10]. The detailed information can be found in Table 1. For student models, we employed the ResNet-18 [18] and MobileNetV2 [33] architectures.

Evaluation Metrics After training, we evaluate the performance using five metrics: Clean, PGD, AutoAttack (AA) accuracy, mean Gradient Distance (GD), and mean Gradient Cosine similarity (GC). Clean refers to the accuracy of the test dataset. PGD assesses the robustness against 20 steps

Dataset	Teacher(Architecture)	Clean	PGD	AA
CIFAR-10	LTD(WRN-34-10)	85.21	60.89	56.94
	BDM-AT(WRN-28-10)	92.44	70.63	67.31
	IKL-AT(WRN-28-10)	92.16	71.09	67.73
CIFAR-100	LTD(WRN-34-10)	64.07	36.61	30.57
	BDM-AT(WRN-28-10)	72.58	44.24	38.83
	IKL-AT(WRN-28-10)	73.80	44.14	39.18

Table 1. Performance (%) of the teacher models.

of PGD attack following the methodology in [29], while AA evaluates the model’s robustness against the AutoAttack method [10]. All attacks were conducted within an l_∞ -norm bound of 8/255. Two additional metrics are introduced: GD and GC. GD measures the average L2 distance between the input gradients of the teacher and those of the student, thus smaller values are preferred. GC quantifies the cosine similarity between the teacher and student input gradients. As the gradients of the student model align more closely with those of the teacher model, the metric approaches one from zero.

4.2. Main Results

We present the comprehensive results of integrating IGDM into AT and AD methods and their original versions in Table 2 and Table 4. IGDM significantly improves robustness, regardless of the original methods, datasets, student models, or teacher models. IGDM demonstrates notably enhanced AA robustness on the CIFAR-100 dataset, achieving 30.32% on ResNet-18 and 29.52% on MobileNetV2. Interestingly, we also observe a correlation between performance and both GD and GC. To provide a clearer visualization of this relationship, we plot the relationship between GD and robustness as well as GC and robustness in Fig. 4. As the regression lines show, robustness increases as GD decreases, and robustness increases as GC increases. This highlights the positive impact of aligning the gradients between the teacher and student models and supports our analysis in Eq. (12). More importantly, we consistently observe a decrease in GD and an increase in GC when IGDM is applied.

4.3. Simple Inner Maximization with IGDM

Recent AD methods commonly utilize a teacher model for inner maximization [20, 49]. While these approaches improve the robustness of the student, employing the teacher in inner maximization involves considerable time consumption. Specifically, AdaAD utilizes the backward function of the teacher model, leading to increased processing time due to the substantial weight size of the teacher’s architecture. In contrast, IGDM demonstrates strong performance even when employing simple inner maximiza-

Dataset	Method	Teacher models & Evaluation metrics														
		LTD [6]					BDM-AT [39]					IKL-AT [11]				
		Clean	PGD	AA	GD↓	GC↑	Clean	PGD	AA	GD↓	GC↑	Clean	PGD	AA	GD↓	GC↑
CIFAR-10	PGD-AT	84.52	42.80	41.12	0.408	0.382	84.52	42.80	41.12	0.409	0.290	84.52	42.80	41.12	0.409	0.286
	+IGDM	84.20	45.09	43.00	0.188	0.421	84.09	44.58	42.60	0.194	0.328	84.31	45.64	43.21	0.171	0.331
	TRADES	82.46	49.13	47.09	0.124	0.521	82.46	49.13	47.09	0.131	0.425	82.46	49.13	47.09	0.131	0.425
	+IGDM	83.50	54.64	48.83	0.088	0.560	83.07	55.59	49.19	0.104	0.458	83.14	54.91	48.76	0.098	0.455
	ARD	85.04	53.27	49.49	0.051	0.603	85.31	49.16	45.95	0.092	0.381	85.41	49.36	45.32	0.087	0.389
	+IGDM	83.85	54.28	51.09	0.042	0.699	84.65	50.82	46.90	0.079	0.436	84.75	51.47	47.10	0.075	0.445
	IAD	84.33	54.24	50.09	0.047	0.619	84.64	49.09	45.78	0.090	0.403	85.22	49.70	45.96	0.083	0.393
	+IGDM	84.49	56.55	51.09	0.038	0.724	83.30	56.77	50.91	0.059	0.538	83.27	56.20	50.02	0.061	0.518
	RSLAD	83.59	55.98	52.13	0.036	0.754	85.18	52.32	48.95	0.071	0.519	85.55	52.13	48.83	0.069	0.531
	+IGDM	82.96	57.33	53.23	0.034	0.761	84.29	53.75	50.09	0.066	0.536	84.59	53.65	49.83	0.065	0.541
AdaAD	85.13	57.27	53.38	0.030	0.822	86.90	54.27	50.83	0.064	0.573	86.59	54.25	50.86	0.062	0.570	
+IGDM	84.53	57.78	54.06	0.029	0.836	86.03	55.14	51.31	0.063	0.580	86.10	55.41	51.29	0.060	0.587	
CIFAR-100	PGD-AT	55.80	19.88	18.86	0.452	0.389	55.80	19.88	18.86	0.173	0.403	55.80	19.88	18.86	0.460	0.306
	+IGDM	60.49	33.72	28.02	0.086	0.668	61.17	35.11	29.01	0.105	0.555	62.91	35.25	28.89	0.122	0.534
	TRADES	53.56	25.85	22.02	0.178	0.456	53.56	25.85	22.02	0.190	0.375	53.56	25.85	22.02	0.199	0.354
	+IGDM	59.29	32.08	26.10	0.076	0.684	60.88	32.26	25.50	0.094	0.517	62.41	31.79	24.02	0.116	0.467
	ARD	61.34	31.19	25.74	0.108	0.592	61.51	30.23	24.77	0.142	0.439	61.38	27.59	23.18	0.178	0.400
	+IGDM	60.14	33.74	28.30	0.087	0.670	60.28	35.75	29.42	0.100	0.570	61.55	35.24	28.87	0.117	0.546
	IAD	60.12	32.91	26.29	0.102	0.596	59.92	31.47	25.15	0.135	0.443	61.09	29.25	23.61	0.173	0.403
	+IGDM	62.73	33.69	27.49	0.086	0.674	62.99	34.76	27.76	0.104	0.549	64.20	33.71	27.03	0.132	0.506
	RSLAD	60.01	32.39	26.94	0.089	0.658	60.22	32.16	26.76	0.118	0.492	61.18	30.54	25.27	0.147	0.444
	+IGDM	60.43	34.02	28.51	0.077	0.709	62.06	35.67	29.78	0.096	0.582	63.55	35.26	29.10	0.119	0.541
AdaAD	63.34	33.39	27.81	0.077	0.736	64.43	33.21	28.06	0.107	0.567	65.36	32.29	26.89	0.133	0.525	
+IGDM	61.70	34.37	28.83	0.071	0.764	64.44	36.19	30.32	0.093	0.632	66.00	34.47	29.22	0.119	0.582	

Table 2. Adversarial distillation result on ResNet-18 with three teacher models on CIFAR-10 and CIFAR-100. The clean, PGD, and AA each indicate performance (%), and GD and GC are mean gradient distance and mean gradient cosine similarity values, respectively. The numbers in bold indicate improved performance.

Method	AA	GD	GC	T/E
AdaAD	28.06	0.107	0.567	10.62
AdaAD w/o T_{in}	25.62	0.141	0.447	2.26
IGDM _{AdaAD}	30.32	0.093	0.632	11.21
IGDM _{AdaAD} w/o T_{in}	29.34	0.098	0.580	3.36

Table 3. Performance of AdaAD and IGDM_{AdaAD} with different inner loss on CIFAR-100, using the ResNet-18 student and the BDM-AT teacher. The ‘w/o T_{in} ’ indicates the use of PGD for inner loss without the teacher, *i.e.*, inner loss utilizing only the student. ‘T/E’ denotes the time per epoch in minutes.

tion without the teacher model. We measured AA, GD, GC, and time per epoch in Table 3 in both cases, with and without the teacher model in inner maximization. The second row demonstrates a significant drop in robustness

when AdaAD’s outer minimization is retained, but the inner maximization is switched to the PGD attack solely on the student model. However, in the fourth row, employing IGDM_{AdaAD} without the teacher model for inner maximization still achieves superior robustness and gradient matching over AdaAD while reducing training time by threefold. Therefore, utilizing IGDM enables achieving strong robustness with a simple inner loss, reducing training time significantly and offering flexibility by eliminating the need for the teacher model in the inner loss.

4.4. Point-wise alignment

We argue in Eq. (12) that IGDM is helpful for point-wise alignment. To experimentally validate this assertion, we compared the distances between the teacher and the student model. We calculated $D(f_S(\mathbf{x} + \delta), f_T(\mathbf{x} + \delta))$ for three cases: when δ is $\mathbf{0}$, random noise from uniform distri-

Dataset	Method	Teacher models & Evaluation metrics														
		LTD [6]					BDM-AT [39]					IKL-AT [11]				
		Clean	PGD	AA	GD↓	GC↑	Clean	PGD	AA	GD↓	GC↑	Clean	PGD	AA	GD↓	GC↑
CIFAR-10	PGD-AT	83.52	44.47	41.19	0.171	0.505	83.52	44.47	41.19	0.175	0.406	83.52	44.47	41.19	0.175	0.401
	+IGDM	83.37	47.06	43.50	0.107	0.524	83.27	47.12	43.79	0.112	0.423	83.08	47.23	43.46	0.112	0.422
	TRADES	81.57	50.49	46.88	0.062	0.605	81.57	50.49	46.88	0.074	0.492	81.57	50.49	46.88	0.073	0.489
	+IGDM	80.95	52.92	47.97	0.039	0.650	81.17	52.88	47.47	0.051	0.498	80.54	52.65	47.56	0.055	0.491
	ARD	84.18	52.16	48.11	0.054	0.578	84.38	48.26	44.02	0.091	0.371	84.68	48.03	44.11	0.087	0.376
	+IGDM	82.27	53.33	49.93	0.042	0.673	82.13	52.19	47.24	0.067	0.485	81.93	52.21	47.45	0.067	0.489
	IAD	83.38	52.71	48.45	0.051	0.592	83.79	48.36	44.02	0.088	0.385	84.25	48.58	44.15	0.082	0.39
	+IGDM	83.65	54.57	50.14	0.038	0.704	81.07	54.12	48.96	0.059	0.514	81.48	54.34	49.07	0.059	0.515
	RSLAD	82.60	54.55	50.44	0.040	0.706	84.69	50.94	47.38	0.074	0.491	85.36	51.43	47.69	0.072	0.503
	+IGDM	81.97	55.60	51.11	0.039	0.707	84.08	52.65	48.73	0.071	0.501	83.65	53.38	48.65	0.060	0.510
AdaAD	84.24	55.96	51.60	0.034	0.777	85.21	51.45	47.55	0.069	0.516	85.31	52.10	48.03	0.066	0.524	
+IGDM	83.57	56.18	52.15	0.033	0.791	83.47	52.84	49.03	0.062	0.538	83.92	53.17	49.08	0.061	0.541	
CIFAR-100	PGD-AT	59.23	24.04	21.58	0.194	0.486	59.23	24.04	21.58	0.204	0.408	59.23	24.04	21.58	0.211	0.392
	+IGDM	57.40	33.53	27.70	0.080	0.680	57.66	33.83	27.87	0.099	0.548	59.75	33.59	27.02	0.120	0.517
	TRADES	51.05	24.83	20.62	0.119	0.460	51.05	24.83	20.62	0.132	0.377	51.05	24.83	20.62	0.148	0.351
	+IGDM	56.81	29.87	23.38	0.081	0.640	57.80	29.47	22.05	0.097	0.469	59.40	27.83	20.12	0.120	0.417
	ARD	60.55	30.82	25.28	0.111	0.569	61.06	31.25	24.70	0.137	0.445	61.52	28.00	23.40	0.164	0.420
	+IGDM	58.43	33.31	27.86	0.087	0.650	58.81	33.34	27.45	0.111	0.518	60.31	32.54	27.09	0.134	0.492
	IAD	56.11	29.55	24.22	0.106	0.547	56.35	28.96	23.43	0.129	0.430	58.39	28.40	23.06	0.147	0.418
	+IGDM	58.60	31.36	25.64	0.090	0.617	57.65	31.97	25.60	0.106	0.506	59.58	30.96	25.42	0.128	0.478
	RSLAD	60.43	32.37	26.85	0.092	0.632	61.29	31.74	26.18	0.121	0.490	61.95	30.16	25.09	0.157	0.441
	+IGDM	60.36	33.99	28.00	0.079	0.696	60.56	35.24	29.52	0.099	0.571	62.48	35.25	28.82	0.118	0.547
AdaAD	61.43	30.58	25.03	0.091	0.649	61.89	29.54	23.80	0.118	0.497	62.35	28.51	23.01	0.140	0.470	
+IGDM	59.88	32.60	27.01	0.080	0.702	60.58	33.38	26.93	0.097	0.577	61.59	32.43	25.62	0.121	0.531	

Table 4. Adversarial distillation result on MobileNetV2 with three teacher models on CIFAR-10 and CIFAR-100. The clean, PGD, and AA each indicate performance (%), and GD and GC are mean gradient distance and mean gradient cosine similarity values, respectively. The numbers in bold indicate improved performance.

bution, and adversarial perturbation in Table 5. We utilize L2 distance for D . For the adversarial noise, we conducted an adversarial attack using the inner maximization loss corresponding to each method, with a fixed number of steps at 20. In all cases, we observed an improvement in alignment when using IGDM. In particular, IGDM enhanced alignment against not only adversarial noise but also random noise. This outcome shows that our module contributes to point-wise alignment, as demonstrated in Eq. (12).

4.5. Ablation Studies

In this section, we conduct more extensive experiments, including black-box attacks and unseen norm attacks. Here, we chose the CIFAR-100 dataset with ResNet-18 architecture. In the case of the teacher, we selected BDM-AT.

Method	$D(f_S(\mathbf{x} + \delta), f_T(\mathbf{x} + \delta))$		
	$\delta = \mathbf{0}$	$\delta \sim U[-8/255, 8/255]$	$\delta = \text{adv}$
ARD	23.93	23.93	28.49
+IGDM	13.19	13.12	15.33
IAD	23.76	23.74	28.11
+IGDM	13.43	13.42	16.84
RSLAD	19.06	19.02	23.74
+IGDM	12.38	12.33	15.16
AdaAD	18.00	17.94	25.29
+IGDM	12.95	12.94	18.57

Table 5. Point-wise alignment with IGDM on CIFAR-100, using the ResNet-18 student model and the BDM-AT teacher model. The numbers in bold indicate enhanced point alignment.

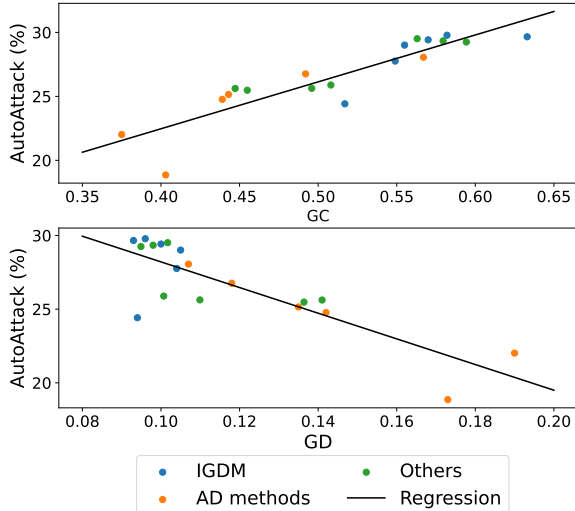


Figure 4. Correlation between GC and AutoAttack (*top*), and correlation between GD and AutoAttack (*bottom*). All results are achieved through different methods with ResNet-18 and a BDM-AT teacher on CIFAR-100. The values for IGDM and AD methods are the same with Table 2. Others represent the results of additional experiments conducted under the same configuration.

Robustness against unseen and black-box attacks To demonstrate that we effectively distill the robustness of a teacher model, we also measured performance against the different attack scenarios in Table 6. First, we assessed the performance against PGD-L1 and PGD-L2 unseen attacks in a white-box setting. We set L1 boundary and L2 boundary as 12 and 128/255, respectively. Experimental results show that adding our module increases performance for both L1 and L2 unseen attacks. Subsequently, we evalu-

Method	Unseen		Black-box
	PGD-L1	PGD-L2	VMI-FGSM
PGD-AT	30.33	28.73	49.18
+IGDM	45.21	42.68	53.54
TRADES	30.82	31.71	48.06
+IGDM	48.75	41.88	50.19
ARD	43.11	39.51	53.57
+IGDM	48.77	43.77	54.20
IAD	39.62	39.37	52.89
+IGDM	45.86	43.57	54.58
RSLAD	41.41	41.05	53.24
+IGDM	44.50	43.76	53.78
AdaAD	44.80	42.45	54.73
+IGDM	45.18	43.76	54.98

Table 6. The robust accuracy of unseen norm attacks and a black-box attack. The numbers in bold indicate improved performance.

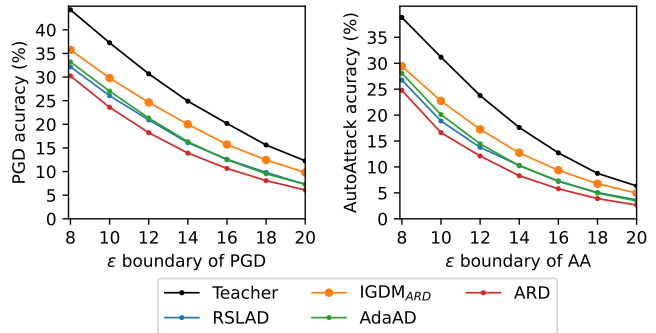


Figure 5. PGD and AutoAttack robust accuracy against stronger attack with larger ϵ boundary. IGDM_{ARD} is implemented for our method.

ated performance against transfer-based black-box attacks. We employed the VMI-FGSM attack method [37] and utilized the ResNet50 model as a surrogate model. We employed an ϵ boundary of 16/255, a commonly utilized value in transfer attacks [13,37,43]. The performance was the best when our module was added to AdaAd as shown in Table 6. Overall, our module improves the performance of existing adversarial distillation methods against various attacks.

Robustness against larger boundary attack In the context of adversarial attacks, an increase of perturbation boundary ϵ corresponds to a stronger attack, leading to lower model robustness against such attacks. However, adversarially well-trained models demonstrate enhanced robustness against attacks with larger perturbation boundaries. To evaluate this, we conducted experiments by training models with the conventional ϵ of 8/255 and testing them with larger perturbation sizes in both PGD and AutoAttack, as illustrated in Fig. 5. Remarkably, when employing IGDM, we observed increased robustness compared to other AD methods. This suggests that IGDM has acquired more resilient features against stronger attacks.

5. Conclusion

We have proposed a novel method Indirect Gradient Distillation Module (IGDM) for adversarial distillation. In contrast to conventional adversarial distillation methods that primarily focus on distilling the logits of the teacher model, we concentrate on distilling the gradient information of the teacher model. Notably, we obtain these gradients indirectly by leveraging the locally linear property, a characteristic of adversarially trained models. Furthermore, IGDM can be seamlessly applied to existing adversarial distillation methods. Extensive experimental results demonstrate that the student model with IGDM successfully follows the gradients of the teacher model, resulting in significantly enhanced robustness.

References

- [1] Maksym Andriushchenko, Francesco Croce, Nicolas Flammarion, and Matthias Hein. Square attack: a query-efficient black-box adversarial attack via random search. In *European conference on computer vision*, pages 484–501. Springer, 2020. [2](#)
- [2] Tao Bai, Jinqi Luo, Jun Zhao, Bihan Wen, and Qian Wang. Recent advances in adversarial training for adversarial robustness. *arXiv preprint arXiv:2102.01356*, 2021. [1](#)
- [3] Yang Bai, Yuyuan Zeng, Yong Jiang, Shu-Tao Xia, Xingjun Ma, and Yisen Wang. Improving adversarial robustness via channel-wise activation suppressing. *arXiv preprint arXiv:2103.08307*, 2021. [2](#)
- [4] Nicholas Carlini and David Wagner. Towards evaluating the robustness of neural networks. In *2017 IEEE Symposium on Security and Privacy (SP)*, pages 39–57. Ieee, 2017. [1](#)
- [5] Yair Carmon, Aditi Raghunathan, Ludwig Schmidt, John C Duchi, and Percy S Liang. Unlabeled data improves adversarial robustness. *Advances in neural information processing systems*, 32, 2019. [1](#)
- [6] Erh-Chung Chen and Che-Rung Lee. LTD: low temperature distillation for robust adversarial training. *CoRR*, abs/2111.02331, 2021. [2](#), [3](#), [5](#), [6](#), [7](#)
- [7] Jeremy Cohen, Elan Rosenfeld, and Zico Kolter. Certified adversarial robustness via randomized smoothing. In *international conference on machine learning*, pages 1310–1320. PMLR, 2019. [1](#)
- [8] Francesco Croce, Maksym Andriushchenko, Vikash Sehwag, Edoardo Debenedetti, Nicolas Flammarion, Mung Chiang, Prateek Mittal, and Matthias Hein. Robustbench: a standardized adversarial robustness benchmark. In *Thirty-fifth Conference on Neural Information Processing Systems Datasets and Benchmarks Track*, 2021. [5](#)
- [9] Francesco Croce and Matthias Hein. Minimally distorted adversarial examples with a fast adaptive boundary attack. In *International Conference on Machine Learning*, pages 2196–2205. PMLR, 2020. [2](#)
- [10] Francesco Croce and Matthias Hein. Reliable evaluation of adversarial robustness with an ensemble of diverse parameter-free attacks. In *International conference on machine learning*, pages 2206–2216. PMLR, 2020. [2](#), [5](#)
- [11] Jiequan Cui, Zhuotao Tian, Zhisheng Zhong, Xiaojuan Qi, Bei Yu, and Hanwang Zhang. Decoupled kullback-leibler divergence loss. *arXiv preprint arXiv:2305.13948*, 2023. [2](#), [3](#), [5](#), [6](#), [7](#)
- [12] Nilaksh Das, Madhuri Shanbhogue, Shang-Tse Chen, Fred Hohman, Li Chen, Michael E Kounavis, and Duen Horng Chau. Keeping the bad guys out: Protecting and vaccinating deep learning with jpeg compression. *arXiv preprint arXiv:1705.02900*, 2017. [1](#)
- [13] Yinpeng Dong, Fangzhou Liao, Tianyu Pang, Hang Su, Jun Zhu, Xiaolin Hu, and Jianguo Li. Boosting adversarial attacks with momentum. In *Proceedings of the IEEE conference on computer vision and pattern recognition*, pages 9185–9193, 2018. [8](#)
- [14] Shangchen Du, Shan You, Xiaojie Li, Jianlong Wu, Fei Wang, Chen Qian, and Changshui Zhang. Agree to disagree: Adaptive ensemble knowledge distillation in gradient space. *advances in neural information processing systems*, 33:12345–12355, 2020. [2](#), [3](#)
- [15] Micah Goldblum, Liam Fowl, Soheil Feizi, and Tom Goldstein. Adversarially robust distillation. In *Proceedings of the AAAI Conference on Artificial Intelligence*, volume 34, pages 3996–4003, 2020. [1](#), [2](#), [3](#), [4](#), [5](#)
- [16] Ian J Goodfellow, Jonathon Shlens, and Christian Szegedy. Explaining and harnessing adversarial examples. *arXiv preprint arXiv:1412.6572*, 2014. [1](#)
- [17] Sorin Grigorescu, Bogdan Trasnea, Tiberiu Cocias, and Gigel Macesanu. A survey of deep learning techniques for autonomous driving. *Journal of Field Robotics*, 37(3):362–386, 2020. [1](#)
- [18] Kaiming He, Xiangyu Zhang, Shaoqing Ren, and Jian Sun. Deep residual learning for image recognition. In *Proceedings of the IEEE conference on computer vision and pattern recognition*, pages 770–778, 2016. [5](#)
- [19] Geoffrey Hinton, Oriol Vinyals, and Jeff Dean. Distilling the knowledge in a neural network. *arXiv preprint arXiv:1503.02531*, 2015. [1](#)
- [20] Bo Huang, Mingyang Chen, Yi Wang, Junda Lu, Minhao Cheng, and Wei Wang. Boosting accuracy and robustness of student models via adaptive adversarial distillation. In *Proceedings of the IEEE/CVF Conference on Computer Vision and Pattern Recognition*, pages 24668–24677, 2023. [1](#), [2](#), [4](#), [5](#)
- [21] Mingi Ji, Byeongho Heo, and Sungrae Park. Show, attend and distill: Knowledge distillation via attention-based feature matching. In *Proceedings of the AAAI Conference on Artificial Intelligence*, volume 35, pages 7945–7952, 2021. [1](#)
- [22] Gaojie Jin, Xinpeng Yi, Wei Huang, Sven Schewe, and Xiaowei Huang. Enhancing adversarial training with second-order statistics of weights. In *Proceedings of the IEEE/CVF Conference on Computer Vision and Pattern Recognition*, pages 15273–15283, 2022. [2](#)
- [23] Gaojie Jin, Xinpeng Yi, Dengyu Wu, Ronghui Mu, and Xiaowei Huang. Randomized adversarial training via Taylor expansion. In *Proceedings of the IEEE/CVF Conference on Computer Vision and Pattern Recognition*, pages 16447–16457, 2023. [1](#), [2](#)
- [24] Jangho Kim, Minsung Hyun, Inseop Chung, and Nojun Kwak. Feature fusion for online mutual knowledge distillation. In *2020 25th International Conference on Pattern Recognition (ICPR)*, pages 4619–4625. IEEE, 2021. [1](#)
- [25] Alex Krizhevsky, Geoffrey Hinton, et al. Learning multiple layers of features from tiny images. 2009. [5](#)
- [26] Qizhen Lan and Qing Tian. Gradient-guided knowledge distillation for object detectors. *arXiv preprint arXiv:2303.04240*, 2023. [2](#), [3](#)
- [27] Lin Li and Michael Spratling. Data augmentation alone can improve adversarial training. *arXiv preprint arXiv:2301.09879*, 2023. [2](#)
- [28] Xingjun Ma, Yuhao Niu, Lin Gu, Yisen Wang, Yitian Zhao, James Bailey, and Feng Lu. Understanding adversarial attacks on deep learning based medical image analysis systems. *Pattern Recognition*, 110:107332, 2021. [1](#)

- [29] Aleksander Madry, Aleksandar Makelov, Ludwig Schmidt, Dimitris Tsipras, and Adrian Vladu. Towards deep learning models resistant to adversarial attacks. *arXiv preprint arXiv:1706.06083*, 2017. [1](#), [2](#), [5](#)
- [30] Javier Maroto, Guillermo Ortiz-Jiménez, and Pascal Frossard. On the benefits of knowledge distillation for adversarial robustness. *CoRR*, abs/2203.07159, 2022. [1](#)
- [31] Tianyu Pang, Xiao Yang, Yinpeng Dong, Hang Su, and Jun Zhu. Bag of tricks for adversarial training. *arXiv preprint arXiv:2010.00467*, 2020. [1](#)
- [32] Sylvestre-Alvise Rebuffi, Sven Gowal, Dan A Calian, Florian Stimberg, Olivia Wiles, and Timothy Mann. Fixing data augmentation to improve adversarial robustness. *arXiv preprint arXiv:2103.01946*, 2021. [2](#)
- [33] Mark Sandler, Andrew Howard, Menglong Zhu, Andrey Zhmoginov, and Liang-Chieh Chen. Mobilenetv2: Inverted residuals and linear bottlenecks. In *Proceedings of the IEEE conference on computer vision and pattern recognition*, pages 4510–4520, 2018. [5](#)
- [34] Jihoon Tack, Sihyun Yu, Jongheon Jeong, Minseon Kim, Sung Ju Hwang, and Jinwoo Shin. Consistency regularization for adversarial robustness. In *Proceedings of the AAAI Conference on Artificial Intelligence*, volume 36, pages 8414–8422, 2022. [2](#)
- [35] Lean Wang, Lei Li, and Xu Sun. Gradient knowledge distillation for pre-trained language models. *arXiv preprint arXiv:2211.01071*, 2022. [2](#), [3](#)
- [36] Ningfei Wang, Yunpeng Luo, Takami Sato, Kaidi Xu, and Qi Alfred Chen. Does physical adversarial example really matter to autonomous driving? towards system-level effect of adversarial object evasion attack. In *Proceedings of the IEEE/CVF International Conference on Computer Vision*, pages 4412–4423, 2023. [1](#)
- [37] Xiaosen Wang and Kun He. Enhancing the transferability of adversarial attacks through variance tuning. In *Proceedings of the IEEE/CVF Conference on Computer Vision and Pattern Recognition*, pages 1924–1933, 2021. [8](#)
- [38] Yisen Wang, Difan Zou, Jinfeng Yi, James Bailey, Xingjun Ma, and Quanquan Gu. Improving adversarial robustness requires revisiting misclassified examples. In *International Conference on Learning Representations*, 2020. [2](#)
- [39] Zekai Wang, Tianyu Pang, Chao Du, Min Lin, Weiwei Liu, and Shuicheng Yan. Better diffusion models further improve adversarial training. In *International Conference on Machine Learning (ICML)*, 2023. [2](#), [3](#), [5](#), [6](#), [7](#)
- [40] Zeming Wei, Yifei Wang, Yiwen Guo, and Yisen Wang. Cfa: Class-wise calibrated fair adversarial training. In *Proceedings of the IEEE/CVF Conference on Computer Vision and Pattern Recognition*, pages 8193–8201, 2023. [1](#), [2](#)
- [41] Dongxian Wu, Shu-Tao Xia, and Yisen Wang. Adversarial weight perturbation helps robust generalization. *Advances in Neural Information Processing Systems*, 33:2958–2969, 2020. [2](#)
- [42] Cihang Xie, Yuxin Wu, Laurens van der Maaten, Alan L Yuille, and Kaiming He. Feature denoising for improving adversarial robustness. In *Proceedings of the IEEE/CVF conference on computer vision and pattern recognition*, pages 501–509, 2019. [1](#)
- [43] Cihang Xie, Zhishuai Zhang, Yuyin Zhou, Song Bai, Jianyu Wang, Zhou Ren, and Alan L Yuille. Improving transferability of adversarial examples with input diversity. In *Proceedings of the IEEE/CVF conference on computer vision and pattern recognition*, pages 2730–2739, 2019. [8](#)
- [44] Zhendong Yang, Zhe Li, Xiaohu Jiang, Yuan Gong, Zehuan Yuan, Danpei Zhao, and Chun Yuan. Focal and global knowledge distillation for detectors. In *Proceedings of the IEEE/CVF Conference on Computer Vision and Pattern Recognition*, pages 4643–4652, 2022. [1](#)
- [45] Hongyang Zhang, Yaodong Yu, Jiantao Jiao, Eric Xing, Laurent El Ghaoui, and Michael Jordan. Theoretically principled trade-off between robustness and accuracy. In *International conference on machine learning*, pages 7472–7482. PMLR, 2019. [2](#), [5](#)
- [46] Qingzhao Zhang, Shengtuo Hu, Jiachen Sun, Qi Alfred Chen, and Z Morley Mao. On adversarial robustness of trajectory prediction for autonomous vehicles. In *Proceedings of the IEEE/CVF Conference on Computer Vision and Pattern Recognition*, pages 15159–15168, 2022. [1](#)
- [47] Jianing Zhu, Jiangchao Yao, Bo Han, Jingfeng Zhang, Tongliang Liu, Gang Niu, Jingren Zhou, Jianliang Xu, and Hongxia Yang. Reliable adversarial distillation with unreliable teachers. *arXiv preprint arXiv:2106.04928*, 2021. [1](#), [2](#), [5](#)
- [48] Yichen Zhu and Yi Wang. Student customized knowledge distillation: Bridging the gap between student and teacher. In *Proceedings of the IEEE/CVF International Conference on Computer Vision*, pages 5057–5066, 2021. [2](#), [3](#)
- [49] Bojia Zi, Shihao Zhao, Xingjun Ma, and Yu-Gang Jiang. Revisiting adversarial robustness distillation: Robust soft labels make student better. In *Proceedings of the IEEE/CVF International Conference on Computer Vision*, pages 16443–16452, 2021. [1](#), [2](#), [4](#), [5](#)